COMITATO NAZIONALE PER L'ENERGIA NUCLEARE
Laboratori Nazionali di Frascati

LNF-75/7(P)

M. Nigro, P. Spillantini and V. Valente: MULTIPOLE ANALYSIS OF π^+ AND π^0 PHOTOPRODUCTION FROM THRESHOLD TO E_γ = 330 MeV.

Servizio Documentazione
dei Laboratori Nazionali di Frascati del CNEN
Casella Postale 70 - Frascati (Roma)

Nuclear Physics B84 (1975) 201–220. North-Holland Publishing Company

MULTIPOLE ANALYSIS OF π^+ AND π^0 PHOTOPRODUCTION FROM THRESHOLD TO E_γ = 330 MeV

M. NIGRO
Istituto di Fisica dell'Università di Padova e INFN, Padova

P. SPILLANTINI and V. VALENTE
Laboratori Nazionali di Frascati del CNEN, Frascati, Italy

Received 25 July 1974

Abstract: We present results of an energy independent multipole analysis of π^+ and π^0 photoproduction on protons for photon energies between 160 MeV and 330 MeV. Each isospin part of the $l \leqslant 1$ amplitudes has been parametrized; the $l \geqslant 2$ amplitudes have been approximated by the Born terms. Unambiguous solutions for all the multipoles in the whole range of E_γ have been obtained. The continuity of the solutions as functions of the energy is very good.

1. Introduction

In recent years many works have been devoted to a phenomenological determination of photoproduction amplitudes [1–10]. The reason is that information obtained using this approach can help to resolve the ambiguities of theoretical models [11–15]. The main feature of the phenomenological approach is a search for the best statistical description of the experimental situation, starting from the minimum number of reasonable physical hypotheses.

Here we report the results of an analysis which has the following characteristics:

(i) as experimental input for the differential cross sections, the results of a statistical analysis are used [16, 17] *, while for the other quantities all the existing data are employed (see sect. 2);

(ii) the only physical hypotheses adopted are those suggested by the experimental data as discussed in sect. 3;

(iii) the mathematical technique is a statistical method based on a Monte-Carlo procedure, (see subsect. 3.2).

This method has been used to obtain from the π^+ experimental data the preliminary solution of ref. [3]. Other preliminary results, which include also data π^0, are reported in ref. [18].

* More recent data (up to 1973) have been included in the present analysis.

Table 1
Summary of the statistical analysis for π^+ and π^0 cross sections. For each E_γ we report the number of experimental points N, the χ^2 probability $P(\chi^2)$ with respect to the fitting surface and the number, $n(3\sigma)$, of points whose deviation from the fitting surface exceeds three standard deviations

	$\frac{d\sigma}{d\Omega}(\gamma + p \to \pi^+ + n)$			$\frac{d\sigma}{d\Omega}(\gamma + p = \pi^0 + n)$		
E_γ (MeV)	N	$P(\chi^{2(+)})$	$n(3\sigma)$	N	$P(\chi^{2(0)})$	$n(3\sigma)$
157–160	7	0.24	1	6	0.53	
165	17	0.12				
170	19	0.07				
175	27	0.07				
180	29	0.45		7	0.93	
185	48	0.88				
190	30	0.97	1			
195	29	0.57				
200	50	0.50	1	5	0.53	
205	19	0.97				
210	27	0.13		16	0.46	
215	18	0.84				
220	67	0.58		10	0.69	2
225	30	0.41				
230	42	0.02	1	12	0.94	
235	12	0.03				
240	60	0.98		15	0.90	
250	25	0.71		11	0.03	
260	93	0.23		27	0.01	1
270	29	0.19		29	0.46	
280	62	0.88		25	0.64	
290	63	0.02	1	22	1.00	
300	76	1.00		32	0.98	
310	44	0.87		24	0.97	
320	83	0.45		32	0.26	
325	29	0.99				
330	20	0.82		20	1.00	

Here we report the results of the complete analysis from E_γ = 160 to 330 MeV. As shown in sect. 4 we obtain unambiguous solutions for all the multipoles in this range of E_γ; the accuracy of the solutions and their continuity as functions of the energy are very good over the entire range of energies.

2. Experimental data used in the analysis

For the experimental data we refer to the HERA compilation [17].

The measured values of the asymmetry in the photoproduction by polarized γ rays and the recoil nucleon polarization have been used directly. On the other hand, a fitting procedure has been applied to the experimental data to obtain the differential cross sections. The details of the fitting procedure are reported in ref. [16]; here we give only its general ideas and the results. In the first stage, for each energy E_γ, the angular distributions were fitted; then a smoothing in E_γ at fixed angles was made; subsequently, a second angular fit was made. The final result is given by a surface of cross-section values, everywhere continuous and smoothed in angle and energy; for each point the error of the fit is given.

A summary of the results of the fit is reported in table 1. An important physical result of the fit is that, both in π^+ and π^0 photoproduction, no evidence for waves with $l > 1$ is found over the explored energy range, except for those which come from the retardation term in the π^+ photoproduction process.

3.1. Method of analysis

The total photoproduction amplitude has been expanded in multipole amplitudes taking into account multipoles with $l \leqslant 1$, where l is the angular momentum of the pion: amplitudes with $l > 1$ have been included only in the Born approximation.

This physical hypothesis is suggested by the statistical analysis of the experimental data [16], described in subsect. 2.1. We thus write all the experimental quantities for π^0 and π^+ photoproduction processes as functions of the complex amplitudes $E_{0+}^{\pi^0}, M_{1-}^{\pi^0}, E_{1+}^{\pi^0}, M_{1+}^{\pi^0}; E_{0+}^{\pi^+}, M_{1-}^{\pi^+}, E_{1+}^{\pi^+}, M_{1+}^{\pi^+}$.

Each of these amplitudes $A_{l\pm}^{\pi^0}, A_{l\pm}^{\pi^+}$, has the following isospin structure:

$$A_{l\pm}^{\pi^0} = \tfrac{1}{3}\,(3A_{l\pm}^{(0)} + A_{l\pm}^{(\frac{1}{2})} + 2A_{l\pm}^{(\frac{3}{2})}) = \tfrac{1}{3}\,(A_{l\pm}^{(1)} + 2A_{l\pm}^{(3)}), \tag{1}$$

$$A_{l\pm}^{\pi^+} = \frac{\sqrt{2}}{3}\,(3A_{l\pm}^{(0)} + A_{l\pm}^{(\frac{1}{2})} - A_{l\pm}^{(\frac{3}{2})}) = \frac{\sqrt{2}}{3}\,(A_{l\pm}^{(1)} - A_{l\pm}^{(3)}). \tag{2}$$

Assuming the validity of Watson's theorem and taking as known the phase shifts $\delta_{l\pm}^{2T}$ from pion-nucleon scattering [19], the problem is then reduced to that of determining the eight unknown real amplitudes:

$$A_{l\pm}^{2T}: \ \mathrm{Re}\,E_{0+}^{(1)}, \mathrm{Re}\,E_{0+}^{(3)}, \mathrm{Re}\,M_{1-}^{(1)}, \mathrm{Re}\,M_{1-}^{(3)}, \mathrm{Re}\,E_{1+}^{(1)}, \mathrm{Re}\,E_{1+}^{(3)}, \mathrm{Re}\,M_{1+}^{(1)}, \mathrm{Re}\,M_{1+}^{(3)}.$$

3.2. Method of calculation

If $S_i^{(0)}, S_i^{(+)}$, denote the calculated observable quantities, i.e. differential cross section, asymmetry ratio and nucleon polarization for π^0, π^+ photoproduction for each E_γ, then we have tried to minimize, both of the functions:

$$\chi^{2(0)} = \sum_{i=1}^{N^{(0)}} \left[\frac{S_i^{(0)} - f_i^{(0)}}{\epsilon_i^{(0)}} \right]^2 , \tag{3}$$

$$\chi^{2(+)} = \sum_{i=1}^{N^{(+)}} \left[\frac{S_i^{(+)} - f_i^{(+)}}{\epsilon_i^{(+)}} \right]^2 . \tag{4}$$

In (3) and (4) $f_i^{(0)}, f_i^{(+)}$ represent the measured experimental values with erros $\epsilon_i^{(0)}, \epsilon_i^{(+)}$, corresponding to $S_i^{(0)}, S_i^{(+)}$ respectively; $N^{(0)}, N^{(+)}$ are the numbers of π^0 and π^+ data for each E_γ.

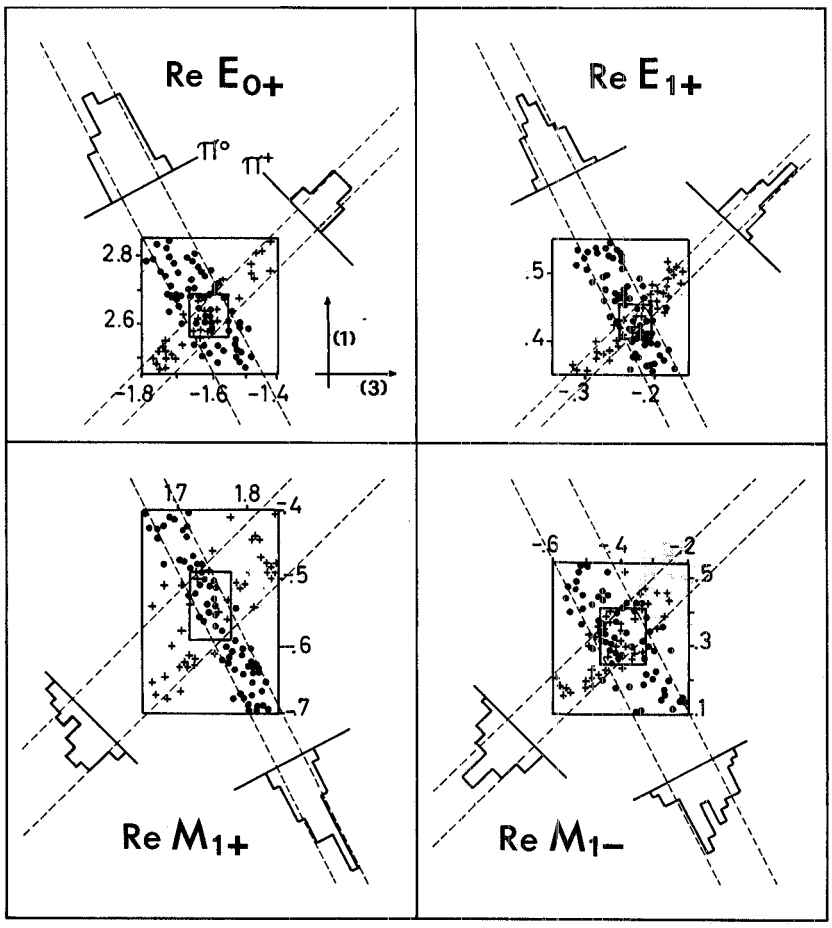

Fig. 1. Two dimensional plot for the determination of the solutions for π^+ and π^0, at $E_\gamma = 220$ MeV. The intersection of the π^+ and π^0 bands defines the region R_i, which contains good solutions for both π^+ and π^0.

A Monte-Carlo program generates a random eight-component vector $A_{l\pm}^{2T}$, and, using (1) and (2), constructs the two four-component vectors $A_{l\pm}^{\pi^0}$, $A_{l\pm}^{\pi^+}$*. The program then calculates $S_l^{(0)}$ and $S_l^{(+)}$ and the values of $\chi^{2(0)}$ and $\chi^{2(+)}$. The ranges over which the multipoles $A_{l\pm}^{2T}$ were varied were two or three times the maximum theoretical uncertainties. If $\chi_T^{2(0)}$, $\chi_T^{2(+)}$ denote two preset values, only those solutions $A_{l\pm}^{2T}$ with $\chi^{2(0)} \leqslant \chi_T^{2(0)}$ are recorded as good solutions for the π^0 process and only those with $\chi^{2(+)} \leqslant \chi_T^{2(+)}$ for the π^+ process.

Due to the large volume of the hyperspace region $\mathcal{A}$ in which $A_{l\pm}^{2T}$ is defined the probability that a random $A_{l\pm}^{2T}$ gives a good solution for π^0 and π^+ stimultaneously is very small.

For each $A_{l\pm}^{2T}$ we construct a two-dimensional plot in which any good solution for π^+ or π^0 is reported as a point $(A_{l\pm}^{(3)}, A_{l\pm}^{(1)})$. The structure of (1) and (2) indicates that the points which come from the π^0 analysis are distributed, in each plot, along the $A_{l\pm}^{(1)} + 2A_{l\pm}^{(3)}$ = constant lines, those coming from π^+ along the $A_{\pm}^{(1)} - A_{l\pm}^{(3)}$= constant lines. Obviously along these lines the value of the imaginary part of the multipole varies. So, if the imaginary parts are small, i.e. the phase shifts are small, representative points of the good solutions are uniformy distributed along these lines.

An example of this case, for E_γ = 220 MeV, is given in fig. 1. At this energy all phase shifts are smaller than 10°. Uniformity in the distribution of points is obtained even if the two phase shifts $\delta_{l\pm}^{\frac{1}{2}}$, $\delta_{l\pm}^{\frac{3}{2}}$, corresponding to the same amplitude $A_{l\pm}$, are equal; in fact, in this case, the imaginary part does not depend on the isotopic components $A_{l\pm}^{(1)}$, $A_{l\pm}^{(3)}$, but only on the combinations (1) or (2).

Conversely, when the phase shift $\delta_{l\pm}^{2T}$ becomes large, the measurable quantities depend strongly on the imaginary part of the $A_{l\pm}^{2T}$ multipole. Therefore limitations on the isotopic part are introduced, and the plot is distorted. As an example of this case, fig. 2 shows the $(M_{1+}^{(3)}, M_{1+}^{(1)})$ plot at E_γ = 320 MeV, where δ_{33} approaches 90° and $M_{1+}^{(3)}$ is resonant.

The intersection of the π^0 and π^+ regions (see fig. 1) is a region $R_i (i = 1, 4)$, which contains good solutions for both π^0 and π^+. The R_i define the projections on the plane of the multipole of the hypervolume $\mathcal{R}$ (of the hyperspace $\mathcal{A}$) in which each eight component vector $A_{l\pm}^{2T}$ represents a good solution of the problem. From the density of points in the R_i regions we determine the mean value for each amplitude and its error.

The advantage of this calculation procedure is that we extract the random $A_{l\pm}^{2T}$ vector in an eight-dimensional space, but the calculation is reduced initially to the two parallel calculations for the $A_{l\pm}^{\pi^0}$ and $A_{l\pm}^{\pi^+}$ vectors, each defined in a four-dimensional space. The final solution for $A_{l\pm}^{2T}$ is obtained as the intersection of $A_{l\pm}^{\pi^0}$ and $A_{l\pm}^{\pi^+}$. For each energy we iterated the calculation, reducing the range of variability of $A_{l\pm}^{2T}$ and the values of the preset $\chi_T^{2(0)}$, $\chi_T^{2(+)}$. The final results apply to a situation

* For the calculation of the imaginary part of $A_{l\pm}^{2T}$ and then of $A_{l\pm}^{\pi^0}$ and $A_{l\pm}^{\pi^+}$, we use the phase shifts of πN scattering from ref. [19].

Table 2
Numerical results for the real parts of the multipole amplitudes having the two isotopic components $A_{l\pm}^{(1)} = 3A_{l\pm}^{(0)} + A_{l\pm}^{(\frac{1}{2})}$ and $A_{l\pm}^{(3)} = A_{l\pm}^{(\frac{3}{2})}$. The multipoles are in units of $10^{-2}\pi$

E_γ	$E_{0+}^{(1)}$		$E_{0+}^{(3)}$		$E_{1+}^{(1)}$		$E_{1+}^{(3)}$		$M_{1+}^{(1)}$		$M_{1+}^{(3)}$		$M_{1-}^{(1)}$		$M_{1-}^{(3)}$	
160	3.13	3.29	−1.98	−1.86	0.12	0.36	−0.19	−0.05	−0.33	0.39	0.23	0.67	−0.16	0.73	−0.59	0.00
170	3.31	3.47	−2.06	−1.96	0.20	0.35	−0.20	−0.09	−0.23	0.31	0.45	0.75	0.21	0.87	−0.60	−0.18
180	3.26	3.36	−1.96	−1.88	0.29	0.36	−0.18	−0.13	−0.27	0.12	0.72	0.92	0.26	0.64	−0.50	−0.25
190	3.14	3.28	−1.85	−1.74	0.30	0.45	−0.25	−0.13	−0.30	0.02	0.95	1.13	0.20	0.65	−0.62	−0.30
200	2.93	3.08	−1.74	−1.59	0.35	0.45	−0.24	−0.16	−0.46	−0.29	1.27	1.36	0.19	0.36	−0.55	−0.22
210	2.78	2.94	−1.65	−1.51	0.38	0.45	−0.24	−0.18	−0.50	−0.37	1.49	1.59	0.17	0.52	−0.57	−0.23
220	2.56	2.69	−1.66	−1.55	0.40	0.45	−0.25	−0.21	−0.59	−0.49	1.72	1.78	0.25	0.41	−0.46	−0.33
230	2.30	2.41	−1.71	−1.63	0.41	0.44	−0.25	−0.23	−0.68	−0.62	1.93	1.97	0.31	0.40	−0.41	−0.34
240	2.08	2.29	−1.76	−1.66	0.38	0.42	−0.27	−0.24	−0.75	−0.70	2.11	2.15	0.32	0.44	−0.37	−0.30
250	2.00	2.14	−1.69	−1.59	0.37	0.41	−0.26	−0.23	−0.73	−0.65	2.30	2.36	0.34	0.45	−0.35	−0.28
260	2.00	2.11	−1.69	−1.59	0.35	0.38	−0.26	−0.24	−0.69	−0.63	2.48	2.52	0.36	0.50	−0.37	−0.28
270	1.95	2.06	−1.58	−1.69	0.33	0.37	−0.24	−0.27	−0.56	−0.61	2.60	2.62	0.34	0.52	−0.28	−0.40
280	1.85	1.96	−1.63	−1.72	0.33	0.37	−0.21	−0.24	−0.55	−0.61	2.61	2.63	0.42	0.58	−0.20	−0.33
290	1.76	1.92	−1.63	−1.77	0.33	0.39	−0.18	−0.21	−0.49	−0.59	2.50	2.55	0.42	0.62	−0.14	−0.29
300	1.66	1.74	−1.73	−1.82	0.34	0.40	−0.14	−0.16	−0.41	−0.47	2.21	2.23	0.54	0.73	−0.02	−0.20
310	1.56	1.69	−1.66	−1.79	0.25	0.37	−0.09	−0.11	−0.39	−0.45	1.81	1.83	0.26	0.52	−0.04	−0.28
320	1.61	1.89	−1.93	−1.72	0.00	0.17	−0.08	−0.06	−0.28	−0.13	1.34	1.38	−0.17	0.12	−0.35	−0.22
330	1.50	1.69	−1.85	−1.72	0.04	0.11	−0.06	−0.05	−0.27	−0.13	0.77	0.78	−0.24	0.04	−0.56	−0.38

Table 3
Numerical results for the real parts of the π^0 multipole amplitudes $A^{\pi^0}_{l\pm}$. The multipoles are in units of 10^{-2} x

E_γ	E_{0+}		E_{1+}		M_{1+}		M_{1-}	
160	−2.58E−01	−1.62E−01	−6.15E−02	6.15E−02	1.20E−01	4.99E−01	−3.48E−01	1.45E−01
170	−2.52E−01	−1.67E−01	−4.94E−02	3.94E−02	2.78E−01	5.47E−01	−2.58E−01	9.81E−02
180	−2.08E−01	−1.45E−01	−1.53E−02	2.53E−02	4.28E−01	6.14E−01	−2.05E−01	4.77E−03
190	−1.70E−01	−8.31E−02	−4.88E−02	4.55E−02	5.66E−01	7.26E−01	−2.95E−01	−3.44E−02
200	−1.64E−01	−5.20E−02	−3.14E−02	3.14E−02	7.10E−01	7.92E−01	−2.78E−01	−5.12E−02
210	−1.54E−01	−4.62E−02	−2.48E−02	2.15E−02	8.41E−01	9.21E−01	−2.81E−01	−5.58E−02
220	−2.37E−01	−1.52E−01	−2.74E−02	4.07E−03	9.60E−01	1.01E + 00	−2.04E−01	−1.02E−01
230	−3.61E−01	−2.98E−01	−2.66E−02	−9.98E−03	1.07E+00	1.10E + 00	−1.59E−01	−1.04E−01
240	−4.65E−01	−3.87E−01	−4.86E−02	−2.46E−02	1.16E+00	1.19E + 00	−1.27E−01	−6.58E−02
250	−4.44E−01	−3.62E−01	−4.58E−02	−2.13E−02	1.30E+00	1.35E + 00	−1.08E−01	−4.86E−02
260	−4.46E−01	−3.70E−01	−5.33E−02	−3.66E−02	1.43E+00	1.46E + 00	−1.11E−01	−3.53E−02
270	−4.62E−01	−3.80E−01	−6.53E−02	−4.13E−02	1.53E+00	1.55E + 00	−1.33E−01	−3.32E−02
280	−5.16E−01	−4.46E−01	−4.53E−02	−2.13E−02	1.54E+00	1.56 + 00	−6.09E−02	4.09E−02
290	−5.73E−01	−4.66E−01	−2.41E−02	4.15E−03	1.48E+00	1.53E + 00	−3.01E−02	9.01E−02
300	−6.49E−01	−5.83E−01	1.13E−02	3.53E−02	1.32E+00	1.34E + 00	7.04E−02	2.06E−01
310	−6.56E−01	−5.59E−01	1.55E−02	5.77E−02	1.06E+00	1.08E + 00	−6.77E−02	1.14E−01
320	−7.17E−01	−5.49E−01	−4.74E−02	1.08E−02	8.09E−01	8.66E−01	−2.63E−01	−1.33E−01
330	−7.11E−01	−6.04E−01	−2.38E−02	4.79E−04	4.26E−01	4.73E−01	−4.22E−01	−2.70E−01

Table 4
The same as table 3 for the real parts of the π^+ multipole amplitudes $A_{l\pm}^{\pi^+}$

E_γ	E_{0+}		E_{1+}		M_{1+}		M_{1-}	
160	2.37E + 00	2.47E + 00	1.04E−01	2.35−01	−3.97E−01	8.96E−04	2.17E−02	5.25E−01
170	2.50E + 00	2.59E + 00	1.54E−01	2.42E−01	−4.10E−01	−1.18E−01	2.54E−01	6.23E−01
180	2.44E + 00	2.50E + 00	2.06E−01	2.47E−01	−5.25E−01	−3.19E−01	2.82E−01	4.96E−01
190	2.32E + 00	2.40E + 00	2.21E−01	3.12E−01	−6.43E−01	−4.70E−01	2.87E−01	5.47E−01
200	2.15E + 00	2.25E + 00	2.53E−01	3.13E−01	−8.42E−01	−7.51E−01	2.24E−01	3.99E−01
210	2.04E + 00	2.14E + 00	2.73E−01	3.16E−01	−9.70E−01	−8.92E−01	2.56E−01	4.70E−01
220	1.95E + 00	2.03E + 00	2.94E−01	3.24E−01	−1.11E + 00	−1.05E + 00	2.93E−01	3.90E−01
230	1.86E + 00	1.93E + 00	3.05E−01	3.22E−01	−1.24E + 00	−1.21E−01	3.17E−01	3.71E−01
240	1.78E + 00	1.85E + 00	2.97E−01	3.21E−01	−1.36E + 00	−1.33E + 00	3.04E−01	3.70E−01
250	1.71E + 00	1.79E + 00	2.88E−01	3.11E−01	−1.45E + 00	−1.40E + 00	3.04E−01	3.65E−01
260	1.71E + 00	1.78E + 00	2.81E−01	2.98E−01	−1.51E + 00	−1.47E + 00	3.17E−01	3.95E−01
270	1.68E + 00	1.75E + 00	2.73E−01	2.97E−01	−1.62E + 00	−1.49E + 00	3.12E−01	4.14E−01
280	1.65E + 00	1.72E + 00	2.59E−01	2.83E−01	−1.52E + 00	−1.49E + 00	3.12E−01	4.09E−01
290	1.62E + 00	1.72E + 00	2.46E−01	2.77E−01	−1.47E + 00	−1.42E + 00	2.88E−01	4.05E−01
300	1.61E + 00	1.67E + 00	2.30E−01	2.60E−01	−1.27E + 00	−1.24E + 00	2.90−01	4.13E−01
310	1.54E + 00	1.62E + 00	1.65E−01	2.22E−01	−1.07E + 00	−1.04E + 00	1.76E−02	3.43E−01
320	1.60E + 00	1.77E + 00	3.27E−02	1.13E−01	−7.74E−01	−7.01E−01	4.77E−02	1.97E−01
330	1.54E + 00	1.65E + 00	4.46E−02	7.79E−02	−4.93E−01	−4.27E−01	9.60E−02	2.53E−01

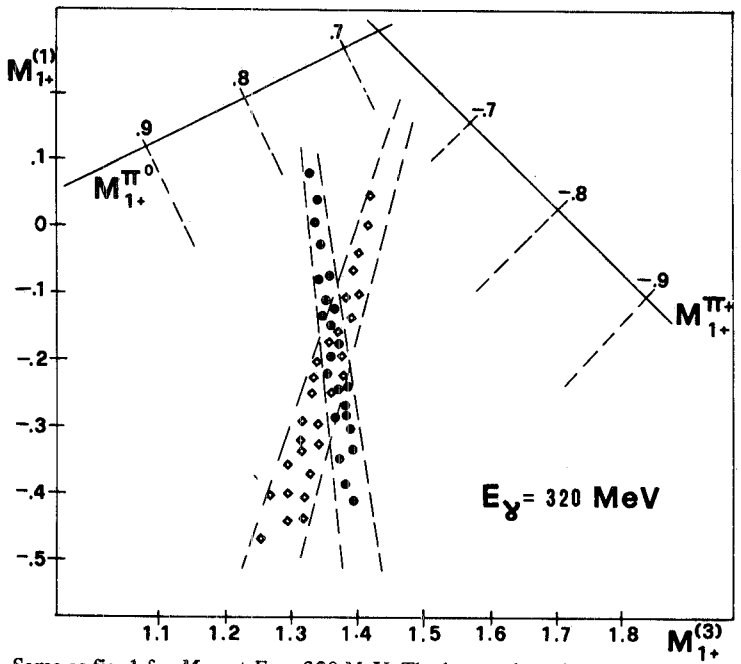

Fig. 2. Same as fig. 1 for M_{1+} at E_γ = 320 MeV. The large value of δ_{33} introduces distorsion in the plot (see text).

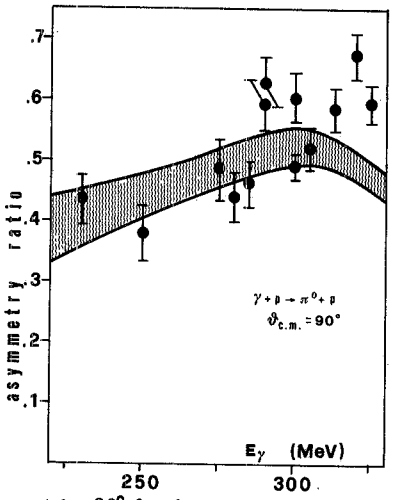

Fig. 3. The excitation curve at $\theta = 90°$ for the asymmetry ratio in π^0 photoproduction by polarized γ rays. The indicated band is calculated taking into account all the uncertainties in the multipole amplitudes of table 1.

in which $\chi_T^{2(0)} \sim N^{(0)}$ and $\chi_T^{2(+)} \sim N^{(+)}$ equal to the number of experimental points. We have obtained solutions for all the amplitudes over the entire energy range investigated, without ambiguities in the values for convergence.

4. Results of the analysis

In table 2 we give the numerical results for the amplitudes in the two isotopic

Table 5

Summary of the statistical significance of the multipole solutions. The table contains, for each E_γ: (i) the number of experimental points N (note that these points are not derived from the fitting procedure of sect. 2 but are taken directly from refs. [17]); (ii) the χ^2 values; (iii) the number of points $n(3\sigma)$ whose deviation from the multipole fit exceeds three standard deviations. The energy-averaged χ^2 probability $P(\chi^2)$, for each measured quantity is also given. Slightly different grouping in energy makes the numbers of experimental points in this table somewhat different from those of table 1.

		$\gamma + p = \pi^+ + n$			$\gamma + p = \pi^0 + n$		
	E_γ	N	$\chi^{2(+)}$	$n(3\sigma)$	N	$\chi^{2(0)}$	$n(3\sigma)$
$\frac{d\sigma}{d\Omega}$	160	16	28.1	2	13	14.8	0
	170	51	73.5	0			
	180	74	71.2	0	16	32.7	0
	190	61	54.3	1			
	200	70	67.8	1	5	1.6	0
	210	45	52.7	0	23	12.8	1
	220	68	75.0	0	9	4.4	1
	225	27	25.8	0			
	230	57	104.4	0	17	8.8	2
	240	61	38.5	0	16	12.9	1
	250	32	34.6	0	10	15.7	1
	260	72	57.9	1	25	25.1	3
	265	19	28.2	0			
	270	29	33.1	0	27	29.1	0
	280	62	40.3	0	28	32.2	0
	290	57	91.5	2	28	24.3	0
	300	72	49.2	0	36	21.3	0
	310	48	43.2	0	24	9.2	0
	320	79	88.1	0	31	30.2	0
	325	28	12.2	0			
	330	14	12.2	0	20	18.5	1
	Total	1041	1073.3	7	328	291.6	10
	$P(\chi^2)$		42.4%			96.4%	
Asymmetry ratio	210–235	32	39.1	1			
	236–284	25	28.3	1	5	4.4	0
	285–330	17	20.7	2	6	23.7	4
	Total	74	88.2	4	11	28.1	4
	$P(\chi^2)$		14.5%			0.3%	
Recoil nucleon polarization	240–330				5	15.9	1
	$P(\chi^2)$					0.7%	

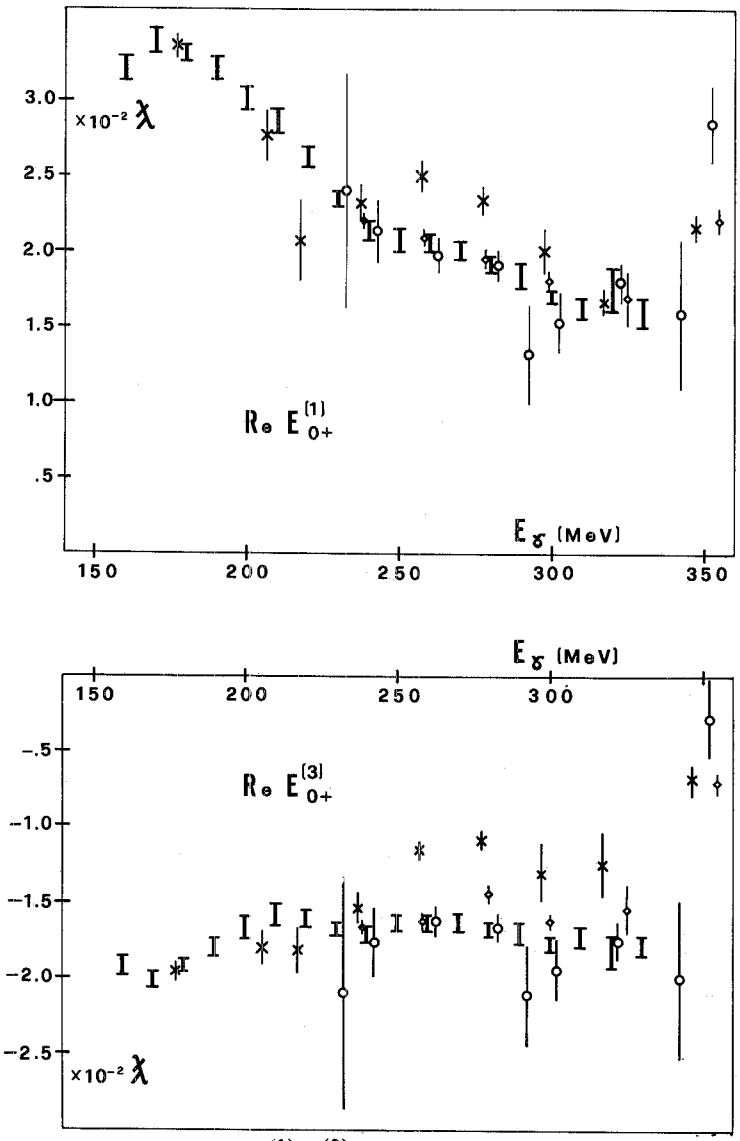

Fig. 4. Results for the real parts of $E_{0+}^{(1)}$, $E_{0+}^{(3)}$ as a function of the photon energy E_γ ⊥ present work, ⊥ ref. [7], ⊥ ref. [8], ⊥ ref. [9].

components $A_{l\pm}^{(1)} = 3A_{l\pm}^{(0)} + A_{l\pm}^{(\frac{1}{2})}$ and $A_{l\pm}^{(3)} = A_{l\pm}^{(\frac{3}{2})}$ at eighteen different energies between 160 and 330 MeV. In tables 3 and 4 we summarize the results for the combined multipoles $A_{l\pm}^{\pi^0}$, $A_{l\pm}^{\pi^+}$. For each amplitude we report the interval that contains about 70% of the good solutions.

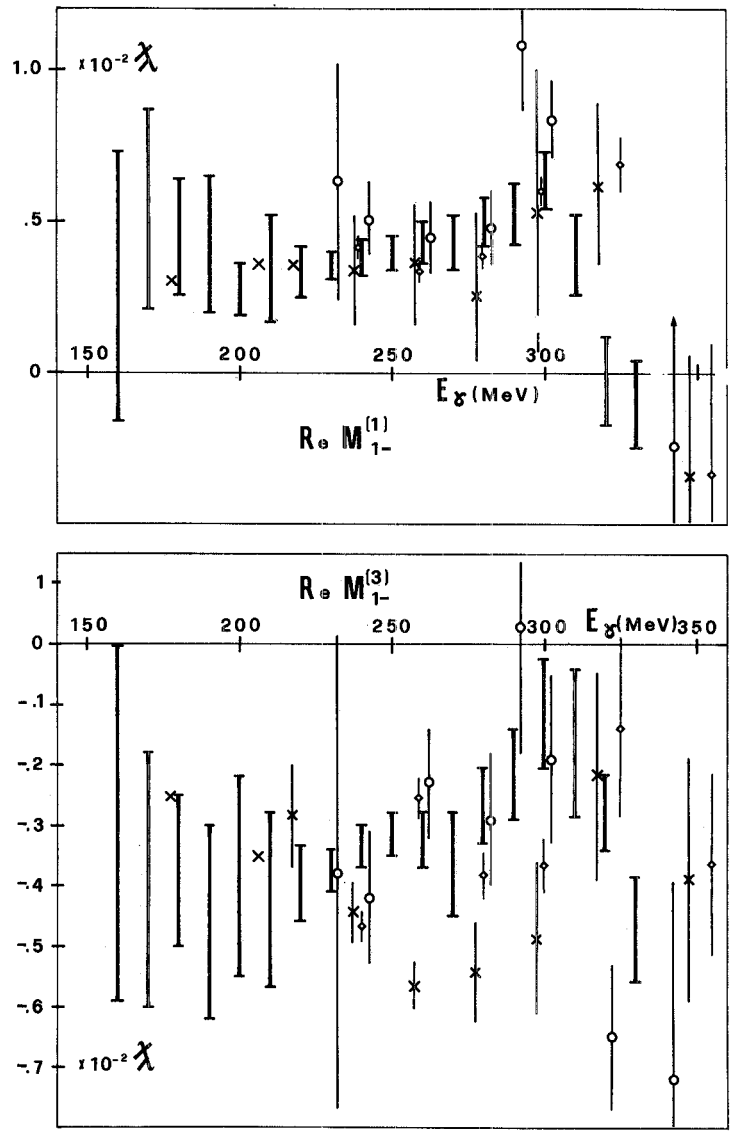

Fig. 5. Same as fig. 4 for $M_{1-}^{(1)}, M_{1-}^{(3)}$.

In order to show the statistical significance for the solutions obtained, we summarize in table 5, for each E_γ, the number of experimental points and the values of $\chi^{2(0)}$ and $\chi^{2(+)}$. The $\chi^{2(0,+)}$ are evaluated according to (3) and (4) introducing into the calculation, for each amplitude, the central value of the intervals given in table 2.

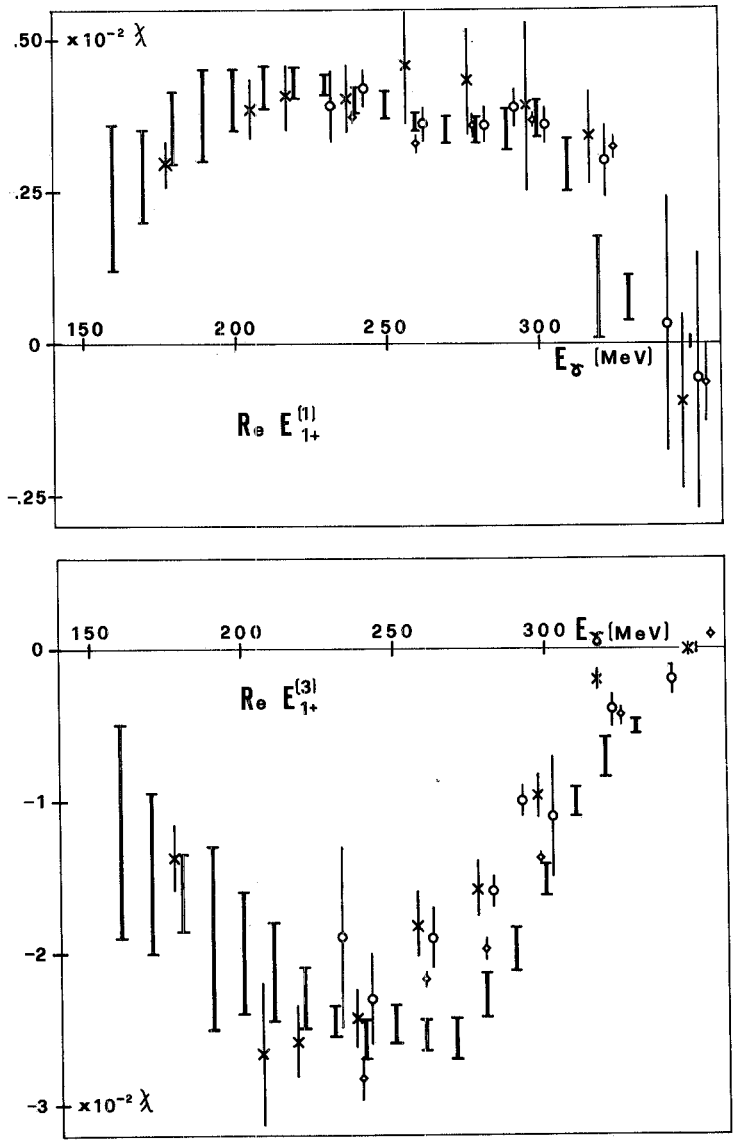

Fig. 6. Same as fig. 4 for $E^{(1)}_{1+}$, $E^{(3)}_{1+}$.

As can be seen from table 5, the solutions reproduce with good accuracy the experimental data for the cross sections of both π^+ and π^0 and for the asymmetry of the π^+. In order to emphasize the discrepancy for the asymmetry of the π^0 (expressed in table 5 by the low χ^2 probability) we present in fig. 3 a comparison between the calculated quantity and the experimental data. The indicated band

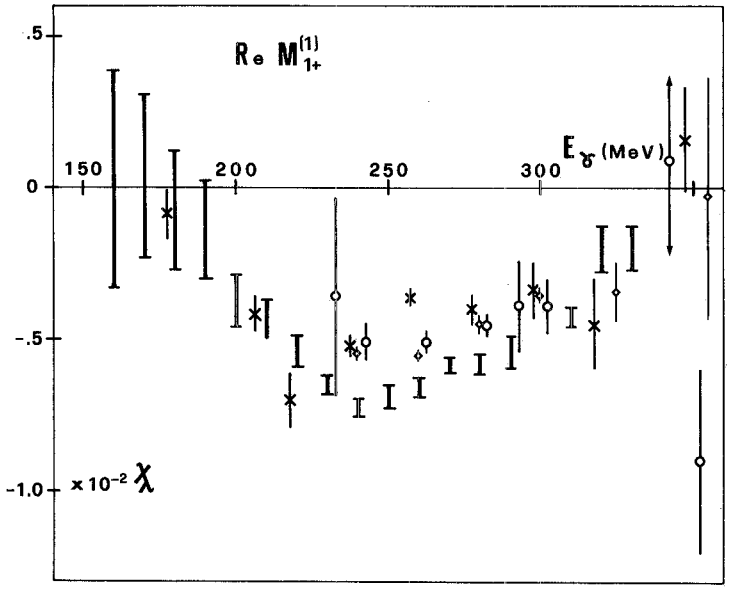

Fig. 7. Same as fig. 4 for $M_{1+}^{(1)}$.

includes all the calculated uncertainties for the multipoles, as reported in table 1. A possible small systematic error (less than 10%) in the experimental points could explain this disagreement. Concerning the recoil nucleon polarization there are few data, so the comparison is not significant. The multipole amplitudes, as functions of the photon energy, are presented in figs. 4–12.

We also studied the dependence of the solutions on the phase shifts using, at some energies, different values for the phase shifts. As an example, in fig. 13 we compare the values of the amplitudes obtained with the phase shifts of ref. [19] and those of ref. [20] at E_γ = 320 MeV. Except for $M_{1+}^{(3)}$, which is very close to the resonant energy and thus is very sensitive to the δ_{33} value, the other amplitudes are unchanged in the limit of accuracy of the results. At lower energies all the amplitudes remain unchanged.

Some general remarks about the results are the following. A peculiar characteristic of our solutions, as shown in figs. 4–12 is their continuity with respect to E_γ; this reflects clearly the fact that the experimental input data are continuous and smoothed in angle and energy.

The general accuracy obtained over the whole range of E_γ is related to the quality of the experimental input data. We remark that the results of refs. [7, 10] were obtained starting from the experimental points, without any analysis of consistency of the whole set of data employed.

A final observation is that the method of calculation used in the analysis was completely statistical. This fact, together with the characteristics of the input data previously discussed, enabled us to obtain unambiguous solutions over the whole range.

In conclusion, we want to point out that our agreement with the results of other authors, refs. [7, 10], is generally good. Therefore, we believe that figs. 4–12 represent the maximum information which can be extracted at this time from the available experimental data on the structure of the π photoproduction amplitude on protons.

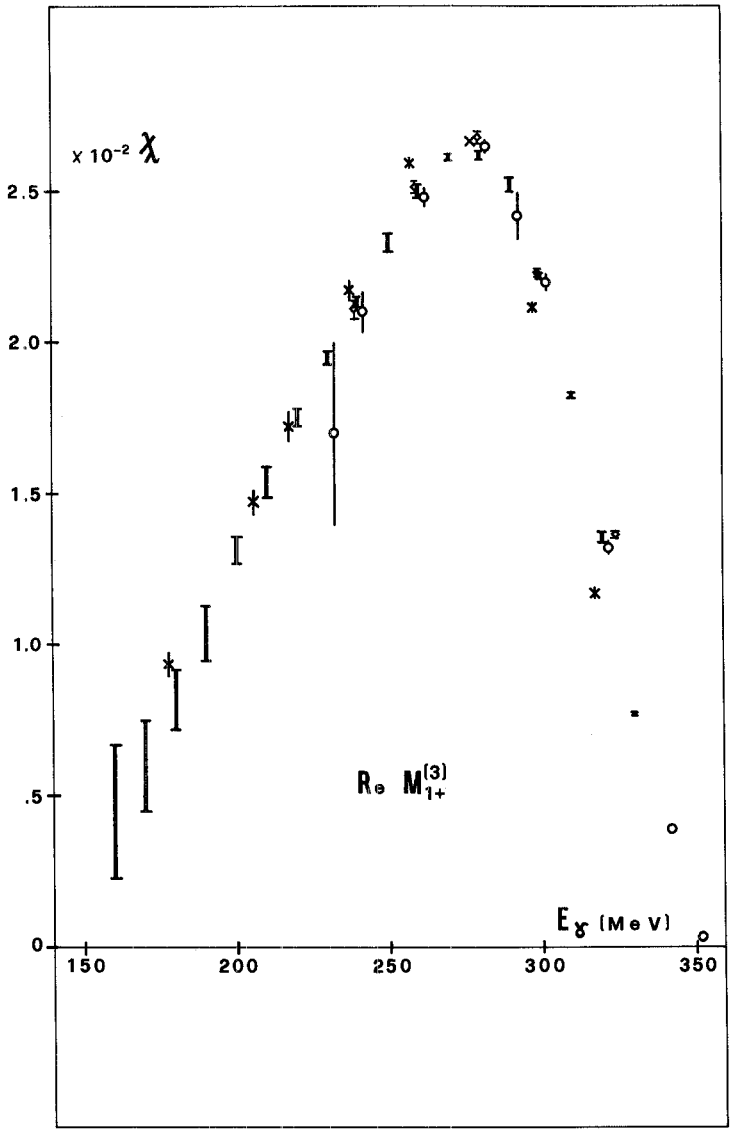

Fig. 8. Same as fig. 4 for $M_{1+}^{(3)}$.

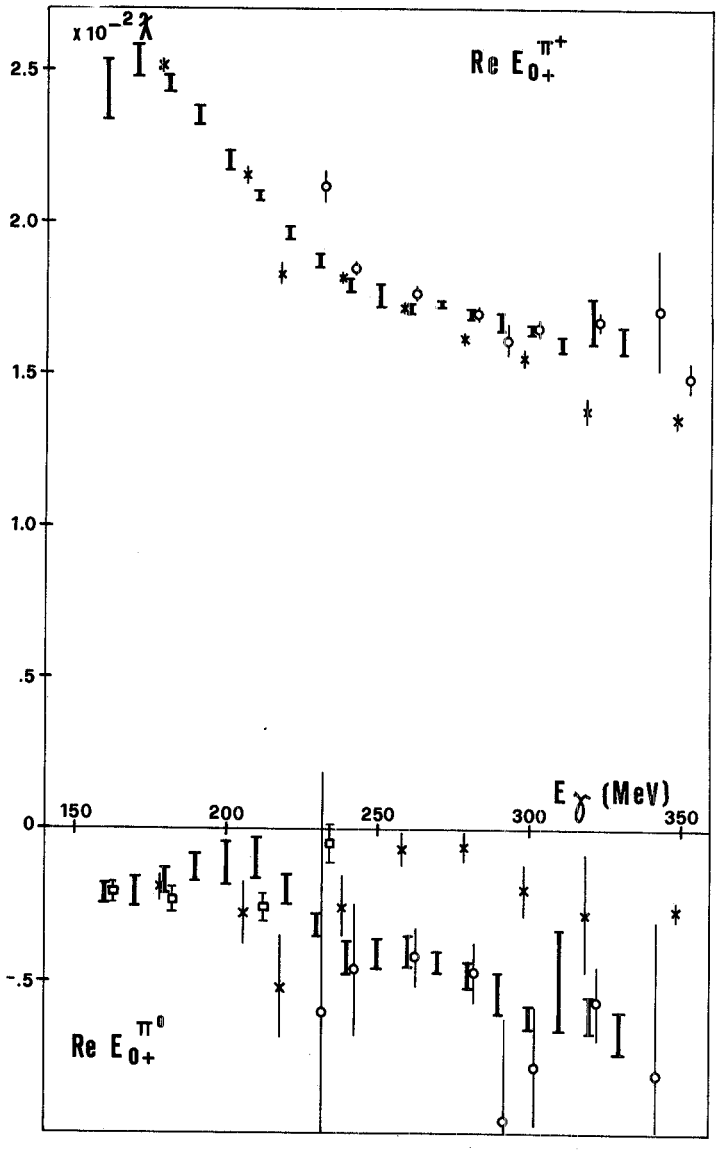

Fig. 9. Results for $E_{0+}^{\pi^+}$ and $E_{0+}^{\pi^0}$ as a function of the photon energy E_γ. ⊥ present work, ⊥ ref. [7], ⊥ ref. [8], ⊥ ref. [10].

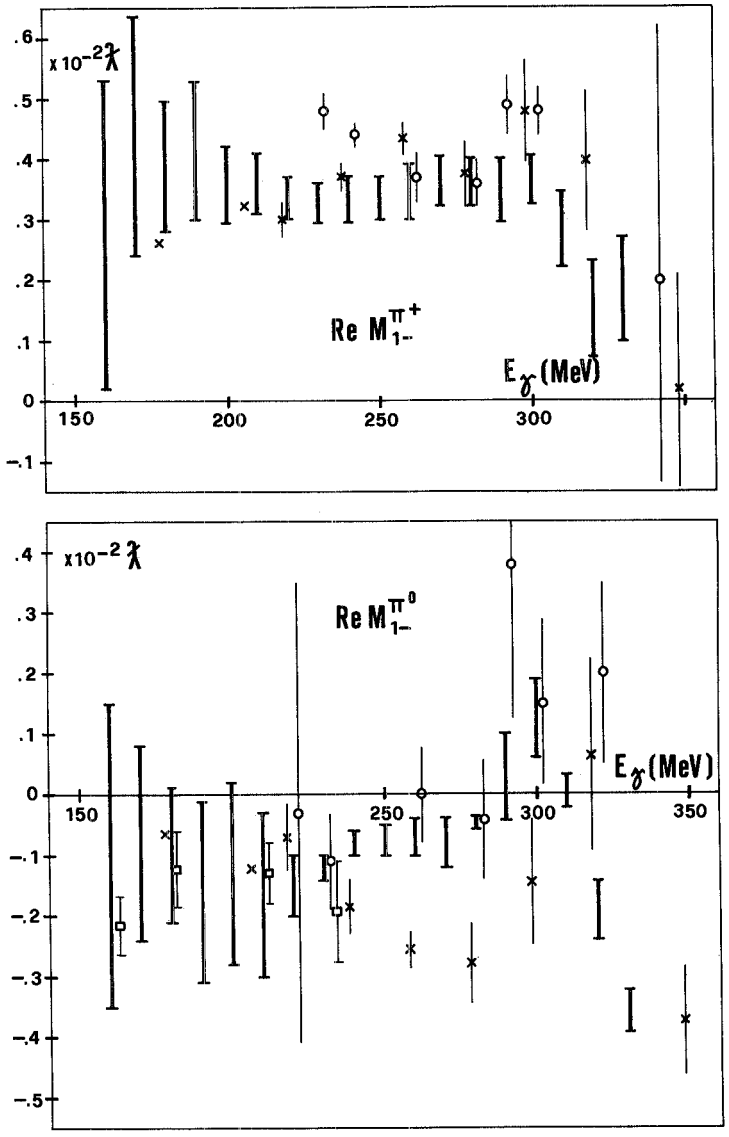

Fig. 10. Same as fig. 9 for $M^{\pi^0}_{1-}$, $M^{\pi^+}_{1-}$.

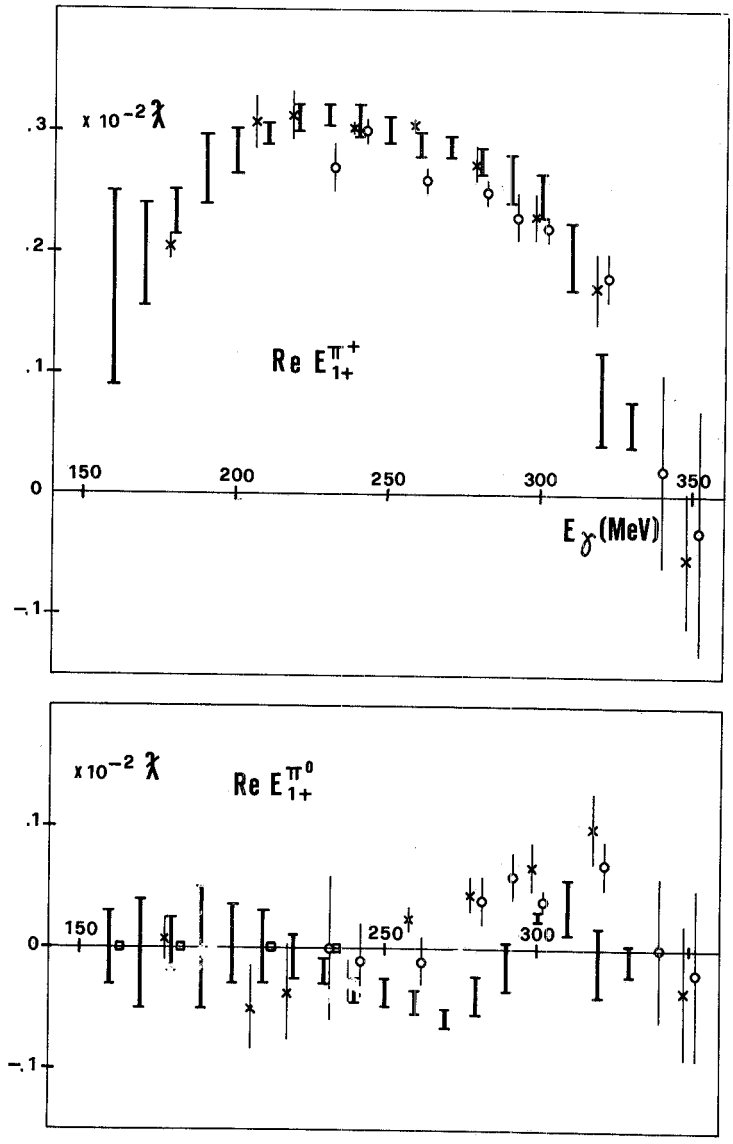

Fig. 11. Same as fig. 9 for $E_{1+}^{\pi^0}$, $E_{1+}^{\pi^+}$.

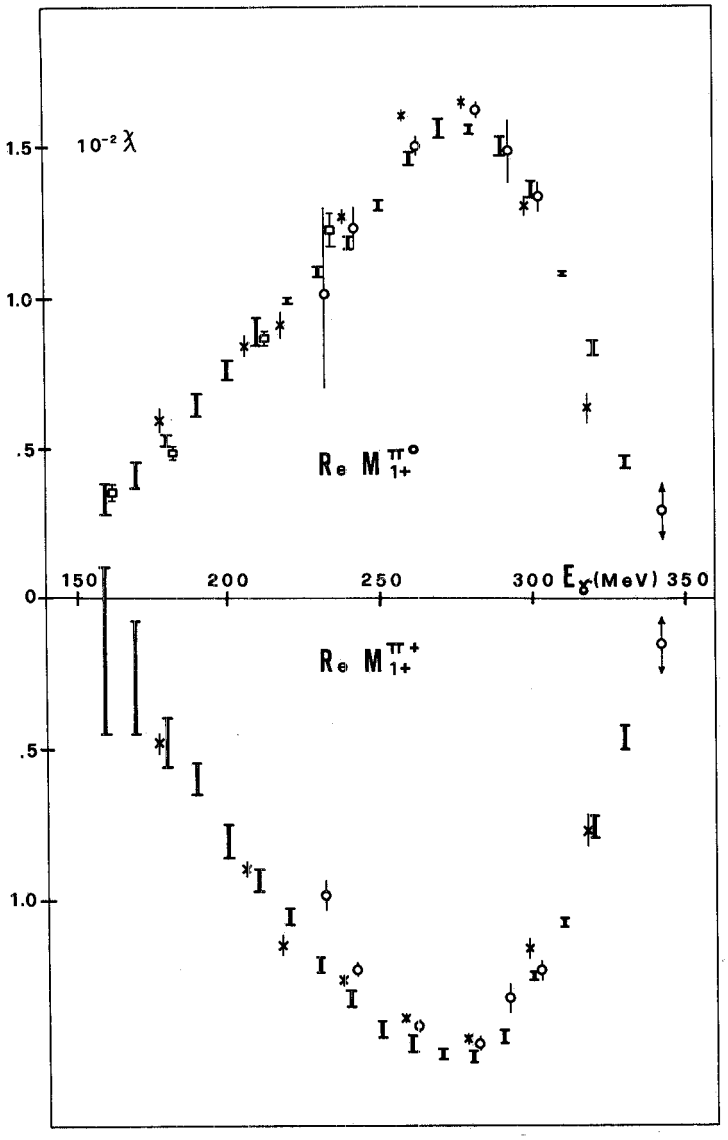

Fig. 12. Same as fig. 9 for $M^{\pi^0}_{1+}$, $M^{\pi^+}_{1+}$.

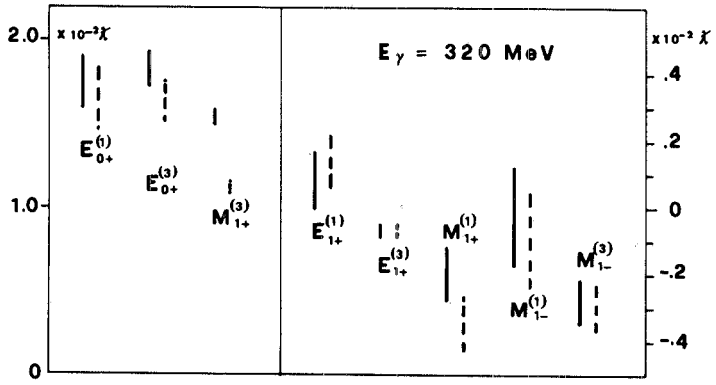

Fig. 13. Comparison of the results of the analysis obtained with the phase shifts of ref. [19] and those of ref. [20], at E_γ = 320 MeV.

References

[1] T. Wennstrom, Nucl. Phys. B5 (1968) 235.
[2] A. Mullensiefen, Z. Phys. 211 (1968) 360.
[3] P. Spillantini, V. Valente, M. Nigro and C. Oleari, Nucl. Phys. B13 (1969) 360.
[4] R.L. Walker, Phys. Rev. 182 (1969) 1729.
[5] P. Noelle, W. Pfeil and D. Schwela, Nucl. Phys. B26 (1971) 461.
[6] F. Berends and D. Weaver, Nucl. Phys. B30 (1971) 575.
[7] W. Pfeil and D. Schwela, Nucl. Phys. B45 (1972) 379.
[8] Y.M. Aleksandrov, V.F. Grushin, E.M. Leikin and A. Ya. Rotvain, Nucl. Phys. B45 (1972) 589; Contribution to the Int. Symposium on electron and photon interactions, Bonn 1973.
[9] S. Suzuki, S. Kurokawa and K. Kondo, Nucl. Phys. B68 (1974) 413.
[10] B.B. Govorkov and E.V. Minarik, Sov. J. Nucl. Phys. 6 (1968) 761.
[11] D. Schwela, H. Rollnik, R. Weizel and W. Korth, Z. Phys. 202 (1967) 451.
[12] J. Engels and W. Schmidt, Phys. Rev. 169 (1968) 1296; 175 (1968) 1951.
[13] D. Schwela and R. Weizel, Z. Phys. 221 (1969) 71.
[14] F.A. Berends, A. Donnachie and D. Weaver, Nucl. Phys. B4 (1969) 1, 54.
[15] G. von Gehlen, Nucl. Phys. B20 (1970) 102.
[16] P. Spillantini and V. Valente, Frascati Internal report LNF 71/28 (1971); LNF 71/93 (1971).
[17] P. Spillantini and V. Valente, CERN-HERA 70/1 (1970).
[18] P. Spillantini, V. Valente, M. Nigro and C. Oleari, Conferenza annuale della Societa Italiana di Fisica, Bari (1969); Contribution to the 15th Int. Conf. on high-energy physics, Kiev 1970.
[19] Particle Data Group, πN partial-wave amplitudes: a compilation, UCRL-20030 πN (1970) 79.
[20] S. Almehed and C. Lovelace, Nucl. Phys. B40 (1972) 157.